Cenozoic evolution of Asian climate and sources of Pacific seawater Pb and Nd derived from eolian dust of sediment core LL44-GPC3

Thomas Pettke and Alex N. Halliday

Federal Institute of Technology, Isotope Geochemistry and Mineral Resources, ETH Zentrum, Zürich, Switzerland

David K. Rea

Department of Geological Sciences, University of Michigan, Ann Arbor, Michigan, USA

Received 6 July 2001; revised 5 April 2002; accepted 5 April 2002; published 27 July 2002.

[1] The large-diameter piston core LL44-GPC3 from the central North Pacific Ocean records continuous sedimentation of eolian dust since the Late Cretaceous. Two intervals resolved by Nd and Pb isotopic data relate to dust coming from America (prior to ~40 Ma) and dust coming from Asia (since ~40 Ma). The Intertropical Convergence Zone (ITCZ) separates these depositional regimes today and may have been at a paleolatitude of ~23°N prior to 40 Ma. Such a northerly location of the ITCZ is consistent with sluggish atmospheric circulation and warm climate for the Northern Hemisphere of the early to middle Eocene. Since ~40 Ma, correlations between Nd ($-7.55 > \varepsilon_{Nd(t)} > -10.81$) and Pb ($18.625 < {}^{206/4}Pb < 18.879$; $15.624 < {}^{207/4}Pb < 15.666$; $38.611 < {}^{208/4}Pb < 38.960$; $0.8294 < {}^{207/6}Pb < 0.8389$; $2.0539 < {}^{208/6}Pb < 2.0743$) isotopes reflect the progressive drying of central Asia triggered by the westward retreat of the paleo-Tethys. Comparisons between the changes with time in the isotopically well-defined dust flux and Nd and Pb isotopic compositions of Pacific deep water allow one to draw two major conclusions: (1) dust-bound Nd became a resolvable contribution to Pacific seawater only after the one order of magnitude increase in dust flux starting at ~3.5 Ma. Therefore eolian Nd was unimportant for Pacific seawater Nd prior to 3.5 Ma. (2) The lack of a response of Pacific deep water Pb to this huge flux increase suggests that dust-bound Pb has never been important. Instead, mobile Pb associated with island arc volcanic exhalatives probably consists of a significant contribution to Pacific deep water Pb and possibly to seawater elsewhere far away from landmasses. *INDEX TERMS:* 0305 Atmospheric Composition and Structure: Aerosols and particles (0345, 4801); 1040 Geochemistry: Isotopic composition/chemistry; 4835 Oceanography: Biological and Chemical: Inorganic marine chemistry; 9355 Information Related to Geographic Region: Pacific Ocean; *KEYWORDS:* neodymium, lead, isotopes, ferromanganese, crust, aerosol

1. Introduction

[2] Past changes in climate, erosion, and atmospheric circulation have been reconstructed from records of eolian dust deposition from sediments of the central ocean gyres, distal to inputs of ash and hemipelagic sedimentation [e.g., *Rea*, 1994]. Complementary constraints on past ocean circulation, erosional regimes on the continents, and hydrothermal inputs at mid-ocean ridges have been obtained from radiogenic isotope time series in hydrogenous marine precipitates, such as ferromanganese crusts. These crusts have monitored the history of the isotopic composition of ambient deep water through time interpreted to result from the complex interplay of many processes including changes in climate and tectonic activity. While isotope tracer compositions of dust are primarily a source indicator [*Taylor et al.*, 1983; *Goldstein et al.*, 1984; *Grousset et al.*, 1988; *Nakai et al.*, 1993; *Jones et al.*, 1994, 2000; *Pettke et al.*, 2000], the deep water isotope signatures have resulted from differences in sources of the input fluxes and redistribution and mixing within the ocean as a function of the respective residence times. Detailed radiogenic isotope stratigraphies from Pacific hydrogenous ferromanganese crusts far from the surrounding landmasses [*Ling et al.*, 1997; *Christensen et al.*, 1997; *Abouchami et al.*, 1997; *Lee et al.*, 1999] have documented changes in radiogenic isotope tracers of ambient Pacific deep water through time, yet the driving forces of these changes have often remained uncertain.

[3] The lack of constraints on isotopic source characteristics and input fluxes of natural Pb is particularly acute because the modern marine cycle of Pb is dominated by anthropogenic Pb, which masks the natural Pb fluxes and isotopic compositions [e.g., *Schaule and Patterson*, 1981]. Lead isotope stratigraphies of ferromanganese crusts far away from continental margins in the central Pacific reveal a component that has been proposed to be eolian in origin [*Jones et al.*, 2000], namely, the portion of Pb loosely bound to eolian dust and released to seawater. In contrast, it was suggested by *von Blanckenburg and Igel* [1999] that the apparently relatively well mixed Pb isotope composition of Pacific seawater results from efficient thermocline mixing, rendering island arc sources for dissolved Pb in the Pacific ocean possible.

0883-8305/02/2001PA000673

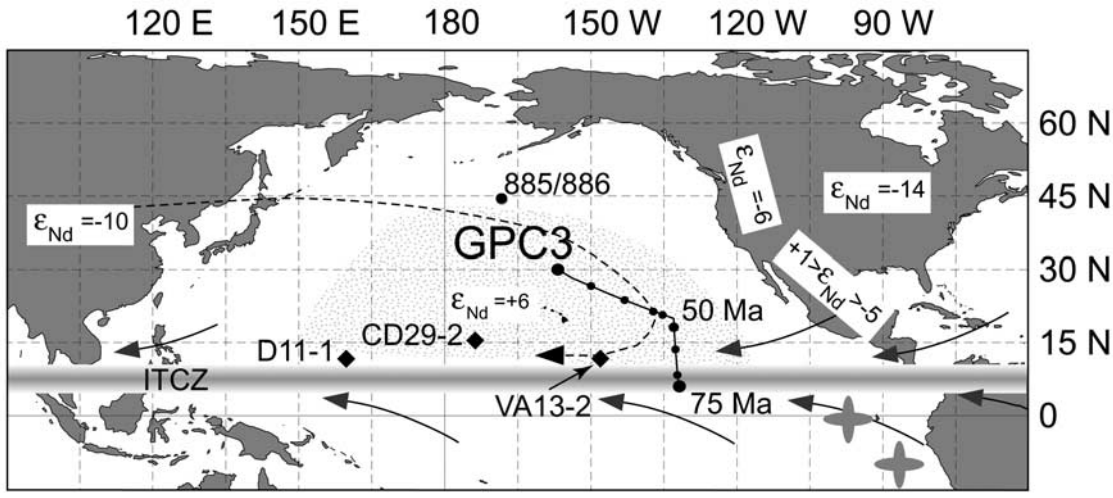

Figure 1. Map of the North Pacific showing the present location of the site of GPC3 together with its corresponding backtrack path [*van Andel et al.*, 1975] where increments of 10 Myr are separated with black dots. Site 885/886 provides a complementary Pb-Nd isotope dust stratigraphy extending back to 11 Ma. Solid diamonds denote sites of ferromanganese crusts D11-1, CD29-2, and VA13-2, respectively. The present-day Intertropical Convergence Zone is shown at ~6°N as a shaded bar together with associated trade winds. The dashed arrow traces modern dust storms emerging from central Asia [*Merrill et al.*, 1989]. The stippled field corresponds to the central North Pacific dust province [*Jones et al.*, 1994]. Neodymium isotopic signatures of dust sources considered in this work are given; crosses west of South America denote turbidite sands and muds with ε_{Nd} values between −5 and +6 [*McLennan et al.*, 1990].

[4] Despite the complementary nature of pelagic dust stratigraphies and ferromanganese crust isotope records covering the entire Cenozoic, there is no direct isotopic comparison available to date between past seawater signatures and corresponding eolian input. The eolian influence on the evolution of seawater isotope chemistry over time has thus remained controversial not only for Pb. It has been argued, for example, that eolian input has no effect on the Nd isotopic budget of seawater [*Jones et al.*, 1994], that it is important for the rare earth element (REE) budget of Pacific seawater [*Greaves et al.*, 1999], or that it constitutes the dominant contribution [*Tachikawa et al.*, 1999].

[5] A continuous record of dust deposition to the North Pacific Ocean extending back to the Late Cretaceous is provided by the well-known large-diameter piston core LL44-GPC3 (hereafter referred to as GPC3), raised from the central gyre region of the North Pacific (Figure 1). Eolian dust accumulation was governed largely by climate and atmospheric circulation patterns superimposed on the motion of the Pacific plate beneath the areas influenced by the different wind belts [*Leinen and Heath*, 1981; *Rea et al.*, 1985]. According to the backtrack path of the location of GPC3 [*van Andel et al.*, 1975] shown in Figure 1, this site has probably moved from a position within the southeast trade winds across the Intertropical Convergence Zone (ITCZ) to a position influenced by northeast trade winds and later to westerly winds at some time in the Cenozoic. This transition is important since the ITCZ separates the hemispheres with respect to dust budget and atmospheric circulation. A band of heavy rainfall associated with the ITCZ effectively washes out the aerosols; hence virtually no dust is transported across the ITCZ [e.g., *Rea*, 1994]. Distinct dust loads thus characterize each hemisphere. On the basis of changes in mineralogy, chemistry, and dust flux [*Corliss and Hollister*, 1982; *Leinen and Heath*, 1981; *Janecek and Rea*, 1983; *Kyte et al.*, 1993] the transition from dust deposited exclusively from westerly winds to dust deposition from easterly trade winds was assigned to some time prior to the Neogene (i.e., >24 Ma), with the notion that andesitic material deposited in the Late Cretaceous and the Paleogene most probably originated from the North and Central Americas. It could not be resolved on the basis of these data, however, if the GPC3 site was ever under the sole influence of Southern Hemisphere winds; hence the paleoposition of the ITCZ throughout the Paleogene has remained uncertain.

[6] Refined geochemical work on bulk GPC3 sediment samples allowed a better resolution of the relative contributions of various sediment sources, the most important ones being eolian, hydrothermal, hydrogenetic, and biogenic [*Leinen*, 1987; *Kyte et al.*, 1993]. Potential sources of eolian particles include central Asia, central North America, Central America, and the northern section of the Andes, which are all characterized by distinct Nd isotopic compositions (Figure 1). On the basis of sediment chemistry, *Kyte et al.* [1993] have proposed that a continental shale-like source component of dust (the continental Eolian 1 component in their Figures 3 and 8) has become progressively more important starting at ~40 Ma until it has fully dominated for the past 10 Myr.

[7] This work aims at constraining the sources of dust deposited in the Pacific Ocean over the past ~70 Myr on the basis of a high-resolution Nd isotope stratigraphy for GPC3 and the time at which the GPC3 site became influenced by

Table 1. Nd Isotopic Data and Sm, Nd Concentrations of Eolian Dust From ODP SITE LL44 GPC3

Sample[a]	mbs[b]	Age (BS),[c] Ma	Age (Co),[d] Ma	Sm, ppm	Nd, ppm	$^{147}Sm/^{144}Nd$ Sample	$^{143}Nd/^{144}Nd$[e,f]	ε_{Nd} modern	$\varepsilon_{Nd(t)}$[f,g]
Surface	0.73	0.29	0.37				0.512121 ± 10	−10.09	−10.08 ± 0.20
55703	3.10	1.44	1.44	3.990	23.703	0.102	0.512083 ± 5	−10.83	−10.81 ± 0.10
55704	3.20	1.51	1.51				0.512092 ± 6	−10.65	−10.61 ± 0.12
55705	3.80	1.98	1.99				0.512084 ± 6	−10.81	−10.76 ± 0.12
55702	3.90	2.06	2.09				0.512124 ± 12	−10.03	−9.97 ± 0.24
55702 duplicate	3.90	2.06	2.09				0.512112 ± 8	−10.26	−10.21 ± 0.16
55707	4.60	3.42	2.93	3.357	19.924	0.102	0.512112 ± 8	−10.26	−10.23 ± 0.16
55708	4.86	4.36	3.51				0.512111 ± 7	−10.28	−10.19 ± 0.14
55709	5.10	5.09	4.12				0.512121 ± 8	−10.09	−9.98 ± 0.16
55710	5.40	6.33	5.02				0.512117 ± 6	−10.16	−10.04 ± 0.12
55711	5.70	7.43	5.93				0.512133 ± 8	−9.85	−9.70 ± 0.16
55712	6.00	8.52	6.76				0.512132 ± 6	−9.87	−9.70 ± 0.12
55713	6.30	9.63	7.40	3.833	22.989	0.101	0.512130 ± 8	−9.91	−9.82 ± 0.16
55714	6.60	10.80	8.45				0.512138 ± 7	−9.75	−9.54 ± 0.14
55714 duplicate	6.60	10.80	8.45				0.512133 ± 7	−9.85	−9.64 ± 0.14
55715	7.20	12.89	10.67				0.512141 ± 5	−9.69	−9.43 ± 0.10
55716	7.40	13.62	11.45				0.512154 ± 5	−9.44	−9.15 ± 0.10
55717	7.70	14.72	12.66				0.512207 ± 6	−8.41	−8.09 ± 0.12
55717 duplicate	7.70	14.72	12.66				0.512195 ± 12	−8.64	−8.32 ± 0.24
55718	7.90	15.45	13.49	2.697	15.746	0.104	0.512208 ± 6	−8.39	−8.23 ± 0.12
55719	8.20	16.54	14.73				0.512179 ± 5	−8.95	−8.58 ± 0.10
55720	8.50	17.64	16.18				0.512230 ± 13	−7.96	−7.55 ± 0.26
55721	9.00	19.46	19.02				0.512212 ± 8	−8.31	−7.83 ± 0.16
55722	9.30	20.55	21.02	2.191	12.787	0.104	0.512213 ± 8	−8.29	−8.04 ± 0.16
55723	9.50	21.28	22.47				0.512206 ± 6	−8.43	−7.86 ± 0.12
55724	9.60	21.64	23.18				0.512204 ± 7	−8.47	−7.88 ± 0.14
55725	10.1	23.47	27.08				0.512215 ± 15	−8.25	−7.57 ± 0.30
55726	10.3	24.20	28.55				0.512180 ± 6	−8.93	−8.22 ± 0.12
55727	10.6	25.30	30.76				0.512191 ± 6	−8.72	−7.95 ± 0.12
55728	10.9	26.39	32.46	1.931	11.666	0.100	0.512199 ± 10	−8.56	−8.16 ± 0.20
55729	11.4	28.22	35.14				0.512173 ± 6	−9.07	−8.19 ± 0.12
55730	11.5	28.58	35.70				0.512169 ± 8	−9.15	−8.25 ± 0.16
55731	11.7	29.30	36.72				0.512143 ± 6	−9.66	−8.74 ± 0.12
55732	12.0	30.40	38.06				0.512144 ± 10	−9.64	−8.68 ± 0.20
55733	12.2	31.13	38.95	1.985	12.889	0.093	0.512118 ± 7	−10.14	−9.63 ± 0.14
55734	12.5	32.22	40.25				0.512144 ± 11	−9.64	−8.63 ± 0.22
55735	12.7	32.95	41.06				0.512174 ± 9	−9.05	−8.02 ± 0.18
55736	12.9	33.71	41.91				0.512190 ± 9	−8.74	−7.69 ± 0.18
55737	13.1	34.76	42.75				0.512281 ± 15	−6.96	−5.89 ± 0.30
55738	13.3	36.03	43.63	0.873	5.273	0.100	0.512296 ± 9	−6.67	−6.13 ± 0.18
55739	13.5	37.30	44.62	1.512	10.003	0.091	0.512120 ± 10	−10.10	−9.50 ± 0.20
55739 duplicate	13.5	37.30	44.62				0.512113 ± 6	−10.24	−9.12 ± 0.12
55740	13.7	38.57	45.50				0.512290 ± 10	−6.79	−5.65 ± 0.20
55741	13.9	39.70	46.31				0.512265 ± 11	−7.28	−6.11 ± 0.22
55742	14.0	40.25	46.70				0.512248 ± 10	−7.61	−6.44 ± 0.20
55743	14.2	41.31	47.42				0.512264 ± 11	−7.30	−6.11 ± 0.22
55744	14.3	41.84	47.80	0.897	5.617	0.097	0.512223 ± 8	−8.10	−7.49 ± 0.16
55745	14.5	42.89	48.45				0.512228 ± 16	−8.00	−6.78 ± 0.32
55746	14.7	43.95	49.13				0.512147 ± 8	−9.58	−8.35 ± 0.16
55747	14.9	44.95	49.83				0.512306 ± 24	−6.48	−5.23 ± 0.46
55747 duplicate	14.9	44.95	49.83	0.799	4.783	0.101	0.512287 ± 8	−6.85	−6.24 ± 0.16
55748	15.2	46.30	51.00				0.512131 ± 9	−9.89	−8.61 ± 0.18
55749	15.4	47.17	51.83	1.400	8.893	0.095	0.512162 ± 12	−9.29	−8.61 ± 0.24
55750	15.7	48.52	53.11				0.512146 ± 9	−9.60	−8.27 ± 0.18
55751	15.9	49.34	53.92	1.440	9.450	0.092	0.512106 ± 6	−10.38	−9.66 ± 0.12
55752	16.2	50.50	55.11				0.512155 ± 10	−9.42	−8.04 ± 0.20
55753	16.4	51.22	55.88				0.512179 ± 7	−8.95	−7.55 ± 0.14
55754	16.7	52.29	56.99				0.512213 ± 12	−8.29	−6.86 ± 0.24
55755	17.0	53.36	57.92	0.655	4.139	0.096	0.512215 ± 13	−8.25	−7.51 ± 0.26
55756	17.2	54.08	58.59				0.512188 ± 9	−8.78	−7.31 ± 0.18
55757	17.5	55.13	59.83				0.512224 ± 25	−8.08	−6.58 ± 0.48
55758	17.8	56.00	61.08				0.512162 ± 8	−9.29	−7.75 ± 0.16
55759	18.1	56.86	62.23	1.061	6.720	0.095	0.512157 ± 8	−9.38	−8.58 ± 0.16
55760	18.5	58.00	63.56				0.512184 ± 11	−8.86	−7.26 ± 0.22
55761	18.7	58.51	63.95				0.512267 ± 12	−7.24	−5.63 ± 0.24
55762	19.0	59.43	64.49				0.512291 ± 20	−6.77	−5.15 ± 0.40
55762 duplicate	19.0	59.43	64.49	0.831	4.950	0.101	0.512276 ± 8	−7.06	−6.28 ± 0.16
55763	19.6	61.14	65.33				0.512201 ± 12	−8.52	−6.89 ± 0.24
55764	20.9	64.77	66.76				0.512250 ± 12	−7.57	−5.89 ± 0.24
55765	21.4	65.88	67.50	0.919	5.425	0.102	0.512300 ± 13	−6.59	−5.78 ± 0.26

Table 1. (continued)

Sample[a]	mbs[b]	Age (BS),[c] Ma	Age (Co),[d] Ma	Sm, ppm	Nd, ppm	$^{147}Sm/^{144}Nd$ Sample	$^{143}Nd/^{144}Nd$[e,f]	ε_{Nd} modern	$\varepsilon_{Nd(t)}$[f,g]
55766	22.3	67.65	69.15				0.512184 ± 10	−8.86	−7.12 ± 0.20
55767	23.2	69.41	70.43	0.808	4.782	0.102	0.512115 ± 14	−10.20	−9.35 ± 0.28

[a] Five digit sample numbers are the University of Rhode Island sample accession numbers.
[b] Here mbs is meters below surface.
[c] Chronostratigraphic age based on ichthyolith biostratigraphy [*Doyle and Riedel*, 1980] as employed by *Janecek and Rea* [1983].
[d] Chronostratigraphic age based on the age model of constant flux of hydrogenous Co [*Kyte et al.*, 1993].
[e] Data are normalized to the natural ratio of $^{143}Nd/^{144}Nd = 0.511847$ [*Wasserburg et al.*, 1981] as further explained in text.
[f] Uncertainties are at the level of 2 standard error of the mean absolute and refer to the least significant digits quoted.
[g] Where not available, a $^{147}Sm/^{144}Nd$ ratio of 0.100 has been employed to calculate the initial ε_{Nd} ratio ($\varepsilon_{Nd(t)}$).

the present-day dominant Asian dust source. The Neogene climatic evolution of central Asia in response to paleogeographic changes and tectonic activity are assessed. Moreover, Nd and Pb isotope data of dust from this core and from site 885/886 [*Pettke et al.*, 2000] located some 1500 km to the NNW allow us to estimate the importance of dust-bound Nd and Pb as a source for the respective isotope budgets of Pacific pelagic seawater.

2. Samples and Analytical Methods

[8] The large-diameter piston core LL44-GPC3 was collected at 30°19.9'N, 157°49.9'W, 5705 m water depth (Figure 1). This site has been out of reach of hemipelagic sedimentation and the occurrence of ice-rafted debris over the entire Cenozoic. Sedimentation rates were between 2 m/Myr (Pleistocene) and 0.2 m/Myr during the early Cenozoic [*Janecek and Rea*, 1983]. Large uncertainties, however, adhere to the chronostratigraphy of the pre-Pliocene section of the core. Ages are only reliable for the top 5 m dated by magnetostratigraphy [*Prince et al.*, 1980] and for the K-T boundary identified at $\sim$ 20.6 m on the basis of high Ir concentrations associated with spheroidal matter and shocked quartz [*Kyte and Wasson*, 1986]. For the period between the Cretaceous-Tertiary boundary and the Pliocene, there are two age models that diverge up to 8 Ma (Table 1). One model is based on ichthyolith biostratigraphy [*Doyle and Riedel*, 1980; *Gottfried et al.*, 1984], which provides

Table 2. Pb Isotopic Data of Eolian Dust From ODP Site LL44 GPC3

Sample[a]	Age,[b] Ma	$^{206}Pb/^{204}Pb$	$^{206}Pb/^{204}Pb$ ±2 SE[c]	$^{207}Pb/^{204}Pb$	$^{207}Pb/^{204}Pb$ ±2 SE[c]	$^{208}Pb/^{204}Pb$	$^{208}Pb/^{204}Pb$ ±2 SE[c]	$^{207}Pb/^{206}Pb$	$^{207}Pb/^{206}Pb$ ±2 SE[c]	$^{208}Pb/^{206}Pb$	$^{208}Pb/^{206}Pb$ ±2 SE[c]
55703	1.44	18.8597	±11	15.6606	±9	38.9597	±22	0.83037	±1	2.06573	±4
55704	1.51	18.7981	±20	15.6538	±17	38.8381	±43	0.83273	±1	2.06607	±4
55705	1.99	18.8677	±23	15.6662	±20	38.9259	±53	0.83031	±1	2.06308	±4
55707	2.93	18.8788	±8	15.6587	±7	38.8905	±20	0.82941	±1	2.05997	±4
55707 duplicate	2.93	18.8764	±15	15.6574	±13	38.8861	±33	0.82975	±1	2.05936	±6
55710	5.02	18.8118	±11	15.6551	±10	38.8826	±27	0.83220	±1	2.06694	±4
55712	6.76	18.8086	±11	15.6546	±9	38.8679	±22	0.83231	±1	2.06646	±4
55713	7.40	18.8076	±9	15.6535	±8	38.8600	±21	0.83230	±1	2.06622	±5
55713 duplicate	7.40	18.8053	±10	15.6503	±8	38.8541	±20	0.83186	±1	2.06450	±5
55718	13.49	18.7221	±9	15.6421	±8	38.7157	±21	0.83550	±1	2.06793	±5
55722	21.02	18.7140	±10	15.6333	±9	38.6684	±27	0.83538	±1	2.06628	±6
55728	32.46	18.8111	±8	15.6365	±6	38.6365	±17	0.83110	±1	2.05391	±4
55730	35.70	18.7481	±18	15.6316	±16	38.6111	±41	0.83377	±2	2.05941	±4
55733	38.95	18.6250	±10	15.6239	±9	38.6331	±23	0.83888	±1	2.07430	±5
55738	43.63	18.5839	±11	15.6234	±11	38.5718	±29	0.84046	±2	2.07554	±5
55738 duplicate	43.63	18.5811	±10	15.6220	±9	38.5656	±24	0.84047	±1	2.07360	±5
55739	44.62	18.6042	±9	15.6158	±8	38.5755	±24	0.83938	±1	2.07348	±5
55744	47.80	18.5750	±9	15.6002	±9	38.4706	±25	0.83985	±1	2.07109	±6
55747	49.83	18.5723	±8	15.6128	±8	38.5522	±23	0.84065	±2	2.07580	±6
55747 duplicate	49.83	18.5728	±10	15.6160	±9	38.5535	±25	0.84081	±1	2.07588	±5
55749	51.83	18.6148	±10	15.6220	±10	38.6035	±27	0.83923	±1	2.07386	±5
55751	53.92	18.6183	±9	15.6208	±8	38.5863	±21	0.83901	±1	2.07248	±4
55755	57.92	18.6069	±9	15.6031	±8	38.4587	±20	0.83856	±1	2.06691	±3
55759	62.23	18.6851	±10	15.6285	±9	38.5747	±23	0.83642	±1	2.06445	±4
55759 duplicate	62.23	18.6818	±12	15.6274	±11	38.5659	±27	0.83659	±1	2.06459	±5
55762	64.49	18.6556	±11	15.6144	±9	38.4777	±24	0.83697	±1	2.06253	±4
55762 duplicate	64.49	18.6606	±21	15.6202	±17	38.4908	±45	0.83708	±1	2.06265	±4
55765	67.50	18.7409	±15	15.6491	±13	38.5895	±34	0.83501	±1	2.05905	±4
55767	70.43	18.8610	±10	15.6593	±8	38.7102	±22	0.83025	±1	2.05193	±5
55767 duplicate	70.43	18.8632	±21	15.6625	±14	38.7149	±41	0.83006	±4	2.05170	±7

[a] Five digit sample numbers are the University of Rhode Island sample accession numbers.
[b] Chronostratigraphic age based on the age model of constant flux of hydrogenous Co [*Kyte et al.*, 1993].
[c] Uncertainties are at the level of 2 standard error of the mean absolute and refer to the least significant digits quoted.

only limited time resolution. The model of constant flux of hydrogenous Co (2.32 mg/(cm Ma) [*Kyte et al.*, 1993]) provides a continuous age versus depth scale that leads to much more detailed mass accumulation rate (MAR) profiles, the accuracy of which, however, is limited by the model assumption. It is important to note that there are no significant indications [*Kyte et al.*, 1993] of any major hiatuses (>5 Myr).

[9] The mineralogy of the bulk sediment, determined by X-ray diffraction, comprises mainly smectite, zeolite, feldspar, subordinate quartz, and traces of mica in the lower section of the core (10–24 m). It changes to illite (50–60%), smectite (20–30%), chlorite, kaolinite, quartz feldspars, and mica in the uppermost 10 m [*Corliss and Hollister*, 1982; *Leinen and Heath*, 1981; *Leinen*, 1987]. All the zeolites and some of the smectites are authigenic, i.e., grew within the sediments by alteration of volcanic material. Authigenic clays would survive the extraction procedure for eolian dust, but examination of the residue of the samples used in this study by scanning electron microscopy (SEM) [*Janecek and Rea*, 1983] shows that authigenic clays are at most a minor component. Moreover, SEM does not reveal diagenetic grain overgrowth. Modeling results [*Leinen*, 1987] suggest that always <3 wt % of the total MAR consists of authigenic components, whereas the detrital fraction has always exceeded 30 wt % of the total sediment. This combined evidence suggests that authigenic clays are a minor component of the samples studied here. Detailed lithological descriptions and a summary of the physical and chemical properties of the GPC3 core are given by *Corliss and Hollister* [1982]. X-ray diffraction mineralogy is given by *Leinen and Heath* [1981] and *Leinen* [1987]. Chemistry is discussed by *Leinen* [1987]. Grain size data are given by *Janecek and Rea* [1983] and *Rea et al.* [1985].

[10] Samples analyzed represent sections of 1 cm of the core. Each data point is thus an integrated representation of ~5000–50,000 years of eolian processes at the observed sedimentation rates [*Janecek and Rea*, 1983]. The samples reflect the input component assemblage at the sea surface [*Rea et al.*, 1985]. Layers that showed the presence of direct deposition of volcanogenic material (most abundant between 9.5 and 13 m [*Corliss and Hollister*, 1982]) were avoided. No attempt was made to analyze direct ashfall deposits as they were thoroughly altered to zeolites, mainly phillipsite [*Leinen*, 1987]; hence the degree of preservation of the original isotopic signatures remains unconstrained.

[11] We analyzed the inorganic silicate fraction of the bulk pelagic sediment, hereafter termed "dust," which was extracted from the bulk pelagic sediment as described by *Janecek and Rea* [1983]. Neodymium isotopic compositions were determined for 65 dust fractions on the basis of which samples were selected for the analysis of Pb isotopic compositions and Sm, Nd, U, and Pb concentrations. The sample size of ~30 mg ensures representative sampling of the dust. The extraction procedure and chemical separation methods are described elsewhere [*Pettke et al.*, 2000]. All analyses were performed by multiple-collector inductively-coupled-plasma mass-spectrometry (MC-ICPMS) (Plasma 54 of VG Elemental®) at the University of Michigan [e.g., *Lee and Halliday*, 1995; *Halliday et al.*, 1998]. Sample solution take-up was in free aspiration mode using an MCN6000 (CETAC Technologies®) desolvating nebulizer. Details of analytical techniques and standard reproducibility are given in Appendix A.

[12] Duplicate runs (marked with duplicate in Tables 1 and 2) for both Nd and the Pb isotopic compositions were identical within the two standard deviation error on the external reproducibility determined on the respective standards, except for the $^{207}Pb/^{206}Pb$ ratio. We attribute this to the combined effect of the very small error we obtained on the $^{207}Pb/^{206}Pb$ reproducibility of the standard (±22 ppm, see Appendix A) combined with a possible small bulk sample heterogeneity. Note that good reproducibility of the Pb isotopic composition was only possible for samples that were allowed to equilibrate the Tl-Pb mixtures for more than a week as documented by *Rehkämper and Halliday* [1999].

3. Results

[13] Neodymium isotopic data for 65 samples and Sm and Nd concentrations for 18 samples of the GPC3 core are tabulated as a function of depth in the core (Table 1). Both currently available age models for this core, ichthyolith biostratigraphy used, for example, by *Janecek and Rea* [1983], and constant flux of hydrogenous Co proposed by *Kyte et al.* [1993], are tabulated in order to highlight the uncertainties associated with the stratigraphic age of a given sample. In this work, we recalculated all sample ages to the model of constant flux of hydrogenous Co to ensure direct age comparability of all data.

[14] Present-day ε_{Nd} values of the dust vary between −6.5 and −10.8; the corresponding ε_{Nd} at the time of sediment deposition (initial ε_{Nd} or $\varepsilon_{Nd(t)}$) varies between −5.8 and −10.8. Two periods can be distinguished in the ε_{Nd} stratigraphy (Figure 2). From 70 to 39 Ma, ε_{Nd} values scatter between −10.2 and −6.5, followed by a smooth evolutionary trend toward more radiogenic values from −10.1 at 39 Ma to −8.0 at 16 Ma. Afterward, the values became less radiogenic approaching the modern ε_{Nd} signature of Asian dust in the late Miocene.

[15] There is no correlation between ε_{Nd} and the dust flux at this site. Samarium and Nd abundances vary between 0.66 and 3.99 and 4.14 and 23.7, respectively, the resulting $^{147}Sm/^{144}Nd$ ratios being uniformly between 0.091 and 0.104 and thus tending to be slightly below those obtained for Site 885/886 [*Pettke et al.*, 2000]. The dust Sm/Nd ratios of around 0.16 are below the mean of 0.195 ± 0.028 of fine-grained sediments (445 isotope dilution analyses of samples of all ages, summarized by *Jahn and Condie* [1995]).

[16] Lead isotopic compositions for 23 samples selected on the basis of the Nd isotope stratigraphy are provided in Table 2 and Figures 3a and 3b. The overall variability of the Pb isotopic compositions is relatively small. The $^{206}Pb/^{204}Pb$ ratios are between 18.57 and 18.88, $^{207}Pb/^{204}Pb$ ratios are between 15.603 and 15.666, $^{208}Pb/^{204}Pb$ ratios are between 38.46 and 38.96, $^{207}Pb/^{206}Pb$ ratios are between 0.841 and 0.829, and $^{208}Pb/^{206}Pb$ ratios are between 2.052 and 2.076.

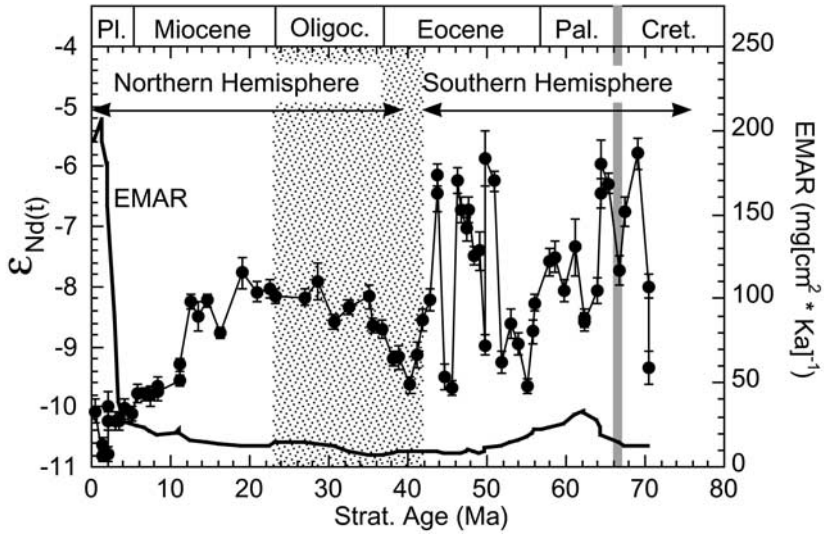

Figure 2. Nd isotope stratigraphy expressed as ε_{Nd} values at the time of dust deposition ($\varepsilon_{Nd(t)}$), related to the three-point smoothed eolian mass accumulation rate (EMAR, dust flux) to the site. The stratigraphy can be divided into two sections, before late Eocene under the likely influence of southeasterly trade winds (Southern Hemisphere) and late Eocene to present with predominance of northeasterly to westerly winds (Northern Hemisphere) for dust transport. The stippled area shows the core interval with layers of direct ashfall deposits.

As with Nd, samples with a stratigraphic age older than ~40 Ma tend to scatter more than younger ones, especially for the $^{206}Pb/^{204}Pb$ and the $^{208}Pb/^{204}Pb$ ratios (Figure 3). Lead isotopic compositions of samples older than circa 30 Ma scatter considerably less than do their corresponding Nd isotopic compositions; hence there is no correlation between ε_{Nd} values and any of the Pb isotope ratios. In younger samples a negative trend has been established, most prominent between ε_{Nd} and $^{207}Pb/^{204}Pb$.

4. Source Constraints for Dust and Central Asian Climate Evolution

[17] The eolian stratigraphy of GPC3 represents a record of dust deposition from various sources because the site migrated beneath different wind belts over time in response to plate motion (Figure 1). Modern sources which contribute to the eolian particles deposited in the central North Pacific north of the present-day ITCZ lie in central Asia and are isotopically well characterized with respect to Nd (Figure 1) and Pb [*Pettke et al.*, 2000; *Jones et al.*, 2000]. According to the backtrack path of the GPC3 site and assuming that the modern situation holds for the Cenozoic, it is likely that this site was south of the ITCZ in early Cenozoic times. Since sources of dust in the Northern and Southern Hemispheres are distinct with respect to Nd isotopic signatures, these can now be used to determine the stratigraphic horizon of the core at which the transition from Southern to Northern Hemisphere influence occurred.

[18] Paleogeographic reconstructions (Paleomap, available at http://www.odsn.de/odsn/services/paleomap/paleomap.html, based on the work of *Hay et al.* [1999]) of the eastern Pacific realm for the Cetaceous-Tertiary boundary show two main features. The western margin of the American continents was essentially established as a coherent subduction zone, with the Caribbean area being covered by seawater except for a few volcanic centers. Volcanic activity in the Central American realm during the past 80 Myr, exceptionally well documented through five drill cores retrieved during ODP LEG 165 [*Sigurdsson et al.*, 1998], is characterized by abundant, large explosive andesitic eruptions. Late Eocene calc-alkaline volcanism associated with this subduction has Sr and Nd isotopic characteristics indicating that the parental andesitic magma consisted of mantle melts (ε_{Nd} of the order of +4 – +8 and unradiogenic Pb) containing a crustal component (unradiogenic Nd, radiogenic Pb) of possibly >20 % [*Wark*, 1991]. Therefore an island arc volcanic component is likely to have been an important source. Another important source was provided by the old basement rocks of South America, continental dust with negative ε_{Nd} values, and radiogenic Pb.

[19] The conspicuous scatter in $\varepsilon_{Nd(t)}$ for GPC3 dust between the Late Cretaceous and middle Eocene may therefore reflect a dominantly binary mixture between pulsed additions of young island arc volcanic material of variable Nd signature from the Caribbean [*Wark*, 1991; *Francis and Hawkesworth*, 1994; *Walker et al.*, 1995; *Petford et al.*, 1996] and a background flux of continental dust. The $\varepsilon_{Nd(t)}$ data reveal that continental dust has always constituted a major fraction of the bulk dust load. Total inversion modeling of end-member source components based on the chemistry of bulk sediment samples [*Kyte et al.*, 1993] suggests a clear trend in the mixture of continental (i.e., shale like) and andesitic (island arc volcanic) material, with volcanic material dominating over shale-like material prior to ~40 Ma. Our Nd data are not in support of the conclusion that volcanic material ever dominated the

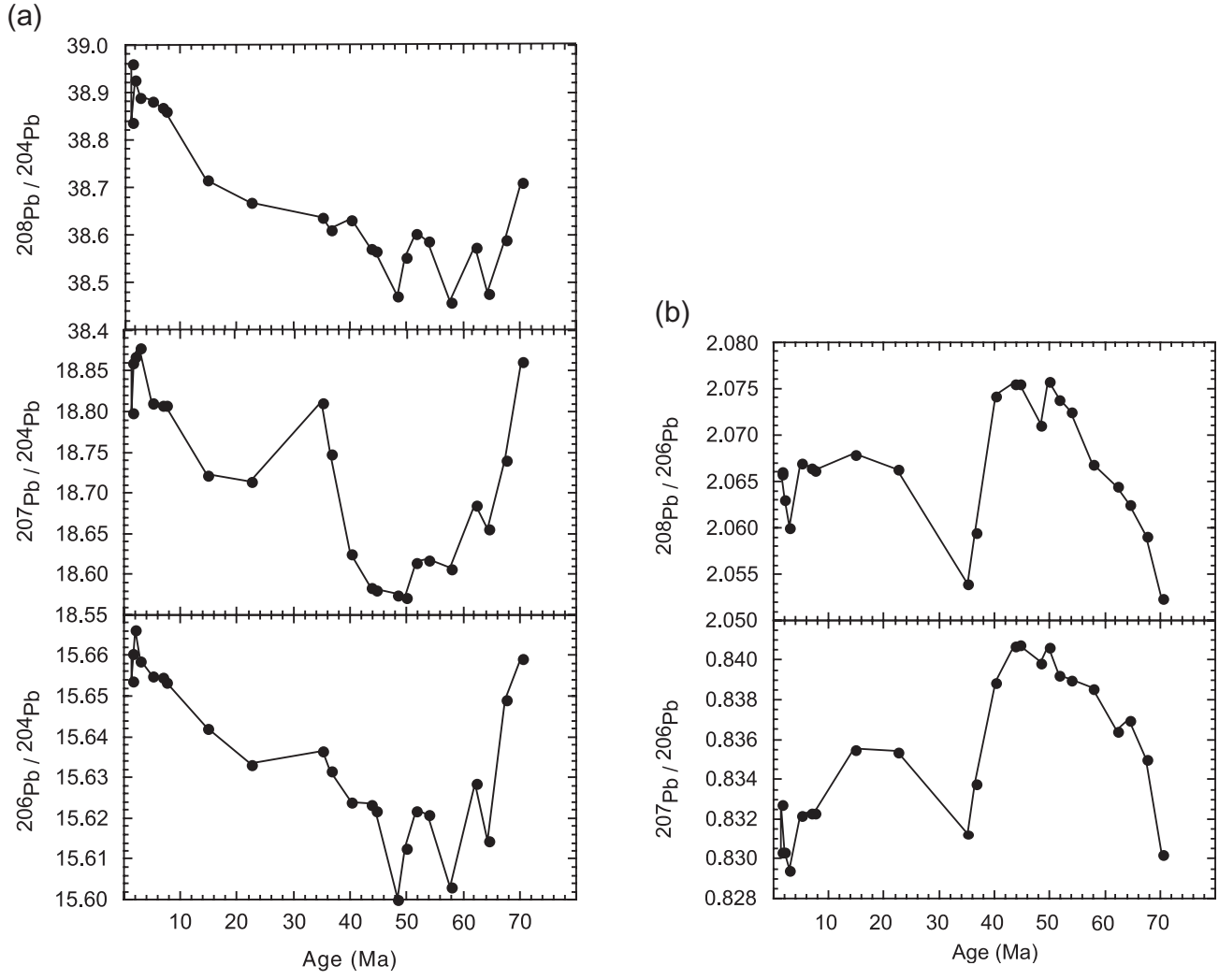

Figure 3. Pb isotope time series of dust deposited at the location of GPC3 through the Cenozoic. (a) The $^{206,207,208}Pb/^{204}Pb$ and (b) $^{207,208}Pb/^{206}Pb$ versus depositional age of the dust.

dust deposited at this site for periods of several million years unless the parental melts assimilated a significant crustal component.

4.1. Dust Deposition From Within the Northern Hemisphere Since ~40 Ma

[20] A striking feature of the isotope record of dust (Figure 2) is the change from scattering $\varepsilon_{Nd(t)}$ values to a smooth trend at ~40 Ma that coincided with a minimum in grain size and is followed by a minimum in dust flux to this site during the late Eocene [*Janecek and Rea*, 1983]. We propose that this section of the core represents the time when the ITCZ migrated relatively southward across the GPC3 site; it thus marks the transition of the site from the Southern Hemisphere wind system to the Northern Hemisphere wind system in the late Eocene. In addition to pure plate motion, a southward shift of the ITCZ is required to account for the observed change in $\varepsilon_{Nd(t)}$ trends because plate motion between circa 43 and 30 Ma was very slow and oblique to latitude (Figure 1). This shift of the ITCZ documents hemispherical changes in climate in the late Eocene. The latitude of the ITCZ is mainly controlled by the relative energies of atmospheric circulation in the hemispheres [*Flohn*, 1981] and therefore implies that the vigor of atmospheric circulation in the Northern Hemisphere increased relative to that of the Southern Hemisphere. At the Eocene-Oligocene boundary the seawater Sr isotopic signature started to become more radiogenic, which possibly could correspond to a feedback on the climatic changes monitored by atmospheric circulation (allowing for the uncertainty inherent in the stratigraphic age of the isotopic shifts monitored by the dust record). The nature of this event, however, cannot be further constrained from available dust data. Clearly, the offset of the ITCZ far into the Northern Hemisphere (~20° in Figure 1; newer models of Pacific plate motion predict 17°–20°N for the paleolatitude of GPC3 at 40 Ma (Paleomap, available at http://www.odsn.de/odsn/services/paleomap/paleomap.html, based on the work of *Hay et al.* [1999]) implies sluggish atmospheric circulation [*Flohn*, 1981], hence

warm conditions, in the Northern Hemisphere for the early to middle Eocene prior to the inferred change in climate.

[21] The Northern Hemisphere record of dust deposition from ~40 Ma to the present is interpreted to contain two principal source contributions, namely, an American andesitic and an Asian shale-like source component. Note that on the basis of Nd isotopic compositions the presence of loess from North America ($\varepsilon_{Nd} = -14$; Figure 1) cannot be confirmed nor rejected but is likely to be unimportant prior to 2.6 Ma. The smooth evolutionary trend of the Nd isotope stratigraphy since 40 Ma contrasts with that of the older section of the core and suggests smoothly evolving mixing proportions. Dust has chiefly been deposited from trade winds during the late Paleogene that also transported direct ashfall deposits from explosive American volcanoes [*Walker et al.*, 1995], observed in the core between 42 and 23 Ma (Figure 2; [*Corliss and Hollister*, 1982]. It can thus be speculated that the trend of increasing $\varepsilon_{Nd(t)}$ values starting at circa 40 Ma reflects a period during which the ITCZ gradually shifted northward from a southern maximum at circa 40 Ma before it shifted gradually southward again starting ~20 Myr ago when less radiogenic $\varepsilon_{Nd(t)}$ values would indicate waning input from North America. It follows that the GPC3 site has probably been dominated by dust deposition from Asia during at least the entire Neogene.

[22] The interpretation presented above is consistent with estimates of the mean annual position of the ITCZ of 10°–12°N in the Miocene [*Flohn*, 1981] and its position of today at ~6°N. It would infer that the latitudinal shift of the ITCZ documented at ~40 Ma was followed by gradual changes over the second half of the Cenozoic. Since the ITCZ shifts into the warmer hemisphere, the deterioration of the Northern Hemisphere climate starting at circa 3.5–4 Ma [*Rea et al.*, 1998] is not reflected in terms of source changes of dust deposited at the GPC3 site. Such an interpretation of the dust record is supported by source component modeling for GPC3 [*Kyte et al.*, 1993] that revealed an almost monotonic increase of a shale-like endmember in the sediment during the past 40 Myr. It has been demonstrated that this shale-like source component has originated from central Asia for the past 11 Myr [*Pettke et al.*, 2000], and it is proposed here that Asian shale-like dust has been a progressively more important source contribution ever since circa 40 Ma.

[23] The Eocene minimum in dust flux and grain size [*Janecek and Rea*, 1983] is consistent with sluggish atmospheric circulation and a humid source, characterized by an $\varepsilon_{Nd(t)}$ signature of about −9. The absence of a clear break in the $\varepsilon_{Nd(t)}$ stratigraphy during the past 40 Myr and progressively better correlation between Nd and Pb isotopic compositions of the dust may be interpreted as evidence for the dominance of a single shale-like source component. In fact, the smoothly evolving $\varepsilon_{Nd(t)}$ values could be explained solely on the basis of a single evolving dust source region in Asia, the interpretation we prefer, without significant continental dust contributions and subordinate andesitic material from North America except the direct ashfall deposits of this time interval. The 40 Ma dust stratigraphy would then reflect the history of progressive desertification and denudation of a single source terrane fairly well mixed with respect to Nd isotopes. If so, the dust flux to the site of GPC3, a proxy for the aridity-humidity levels in the source region, monitors the climatic evolution of central Asia during the past 40 Myr. The absence of Nd isotopic discontinuities at shifts in dust flux (Figure 2) then suggests that the dust stratigraphy records changes in climate in the Asian source terrane, from humid to progressively arid conditions. Such an interpretation agrees well with atmospheric general circulation modeling (GCM) of the Eurasian climate at 30, 10, and 0 Ma by *Ramstein et al.* [1997]. On the basis of realistic continental geography and epicontinental sea distribution in central Asia the westward retreat of the Paratethys has been identified to play a key role in the shift of central Asian climate from Oligocene temperate (oceanic) to continental conditions in the late Miocene. The steady increase of Asian dust flux to the GPC3 site is interpreted to reflect exactly this evolution. Only some 3.5 Myr ago, uplift of the Himalayan-Tibetan Plateau close to modern elevations triggered the desertification of central Asia by changing the pattern of the Asian monsoon [e.g., *Kutzbach et al.*, 1993; *Rea et al.*, 1998] and induced the deterioration of the Northern Hemisphere climate. Then ~2.5 Myr ago the oldest preserved classic Chinese loess deposits accumulated downwind of the central Asian deserts [*Ding et al.*, 1994].

[24] The smooth trend in Nd data during the past 40 Myr further implies that no contamination of the Asian source signal with volcanogenic material from Kamchatka and the Kuril islands has occurred in the late Cenozoic, while such a contamination can be resolved at Site 885/886 for the past 3 Myr [*Pettke et al.*, 2000]. Since Site 885/886 is located some 1500 km to the north of GPC3 (Figure 1), the ε_{Nd} data demonstrate that the central Asian source has dominated dust deposition over the entire central north Pacific north of the ITCZ, by analogy with present-day conditions [e.g., *Merrill et al.*, 1989; *Nakai et al.*, 1993], since the late Eocene. There is no Nd and Pb isotopic evidence for the presence of an 11% Hawaiian source component ($+4 < \varepsilon_{Nd} < +8$ [e.g., *Sims et al.*, 1995]) between 15 and 20 Ma as inferred by *Kyte et al.* [1993] on the basis of geochemical modeling.

4.2. Eolian Dust as a Source for Seawater-Dissolved Pb and Nd?

[25] A growing set of data on the Pb isotopic composition of ancient seawater, chiefly acquired from the analysis of hydrogenous precipitates such as ferromanganese crusts (for the central North Pacific Ocean [*Ling et al.*, 1997; *Christensen et al.*, 1997; *Abouchami et al.*, 1997; *Frank et al.*, 1999]) has revealed regionally distinct patterns and temporal trends. The interpretation of these results, however, is a matter of intense debate, last but not least because the modern global geochemical Pb cycle is dominated by anthropogenic sources [e.g., *Patterson and Settle*, 1987a] that render the direct determination of present-day isotope signatures and fluxes of natural Pb impossible. Recently, it has been proposed that Pb loosely bound to eolian silicate dust has exerted the principal control on the seawater Pb

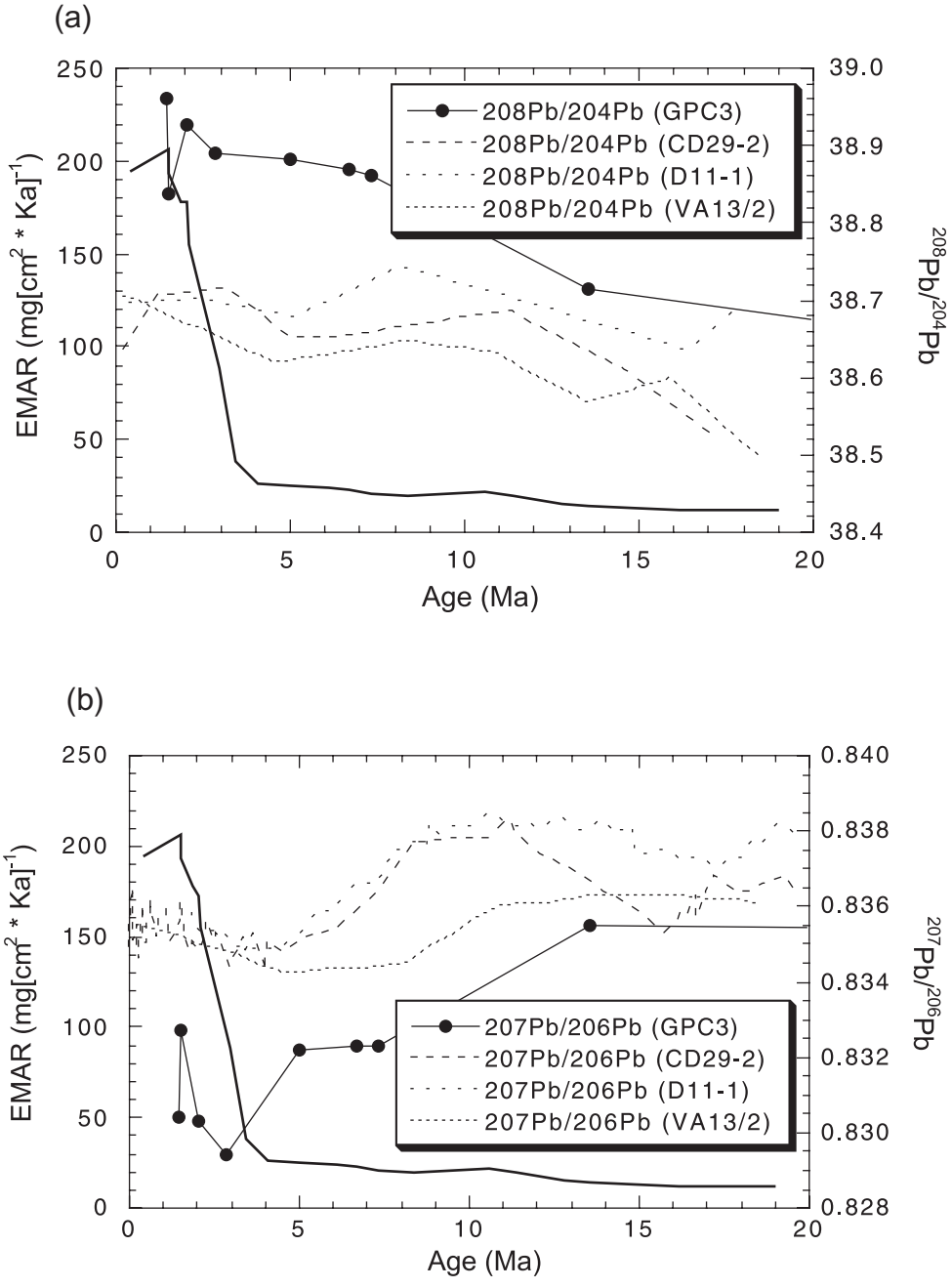

Figure 4. Time series of Pb isotopic compositions of silicate dust (GPC3), Pacific deep water represented by ferromanganese crusts D11-1, CD29-2, and VAl3-2, respectively, and flux of eolian dust (thick solid line) from GPC3. (a) The $^{208}Pb/^{204}Pb$ versus dust flux (EMAR, three-point smoothed) and (b) $^{207}Pb/^{206}Pb$ versus dust flux (EMAR, three-point smoothed) reveal that the central Pacific seawater Pb isotopic composition shows no response to the one order of magnitude increase in dust flux starting 3.5 Ma ago. Possible interpretations for this observation are discussed in text.

isotopic signature for water masses distal to riverine inputs and ocean current advection such as the central North Pacific realm [*Jones et al.*, 2000]. This conclusion is appealing for the modern central North Pacific as it is based on the match of the isotopic signature of exchangeable Pb in Chinese loess and Quaternary seawater Pb from ferromanganese crusts, and it is consistent with the effective removal of river-dissolved and particulate Pb along ocean margins [e.g., *Nozaki et al.*, 1976].

[26] Dust deposited in the central North Pacific since approximately the late Miocene has chiefly originated from a well-mixed source in central Asia [*Pettke et al.*, 2000]. If dust-bound exchangeable Pb is indeed an important source of seawater Pb, the temporal evolution of the

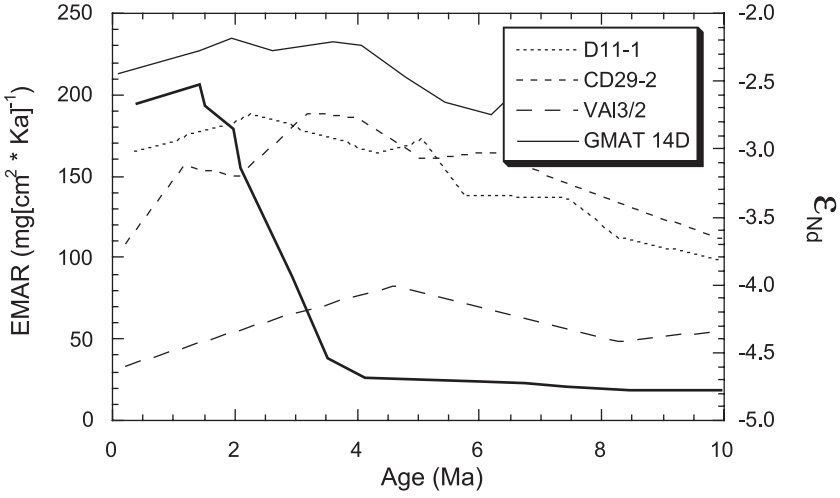

Figure 5. Time series of Nd isotopic compositions of dust (GPC3) and Pacific deep water represented by ferromanganese crusts CD29-2, D11-1, VAl3-2 and GMAT 14D (data are from *Ling et al.* [1997] and *Frank et al.* [1999]) plotted together with dust flux (EMAR, three-point smoothed, thick solid line) to the site of GPC3. The data suggest that dust-bound Nd had a subordinate influence on Pacific seawater Nd only starting 3–4 Myr ago; before that, dust-bound Nd was an unimportant source for seawater-dissolved Nd.

isotopic composition of central North Pacific seawater Pb has to be related to the dust flux as recorded in GPC3 and other central North Pacific sites. Figure 4 shows that the signature of seawater Pb has remained constant while dust flux has increased about one order of magnitude during the latest Cenozoic. Hence either the exchangeable component of eolian dust has no influence on seawater Pb or it completely dominates the signal.

[27] The source of seawater-dissolved Pb (and possibly also the labile component identified by *Jones et al.* [2000]) could be atmospheric of volcanogenic origin. This hypothesis is appealing for several reasons. Much of this Pb is bound in highly soluble species such as volcanic sulfate aerosols [*Patterson and Settle*, 1987a, 1987b]. During preanthropogenic times, about half of the Pb in the troposphere originated from volcanic emissions [*Patterson and Settle*, 1987a, 1987b]. This estimate does not include Pb liberated during eruptions but is based solely on volcanic gas emissions. Volcanic activity along Pacific island arcs intensified significantly at circa 2.6 Ma [*Prueher and Rea*, 2001]; hence the total flux of volcanic Pb is likely to have become even higher. Finally, the Pb isotopic composition of Pacific deep water is similar to that characteristic of Pacific island arc material [e.g., *von Blanckenburg et al.*, 1996]. It is therefore proposed that both the dust-bound exchangeable Pb and the seawater-dissolved Pb originate from atmospheric deposition of Pb liberated through island arc volcanic activity. It is interesting to note that the Pb isotope stratigraphy [*Ling et al.*, 1997] of the northernmost ferromanganese crust in the Pacific, CD29-2, reveals a tendency toward less radiogenic Pb isotope compositions starting at around 3 Ma which could monitor the increase in volcanic eruptions along the Aleutian-Kuriles-Kamchatka arc at this time [*Prueher and Rea*, 2001].

[28] Finally, the data presented here allow one to assess the importance of eolian dust to the Nd budget of Pacific seawater. Figure 5 combines Nd isotopic time series (nonphosphatized) of Pacific ferromanganese crusts with eolian dust flux from Asia for the past 10 Myr. Two features are evident. First, deep water Nd has evolved toward more radiogenic isotopic compositions in the period between 10 and 5 Ma, when dust flux has remained essentially constant. Second, the trends in Nd isotopic compositions of ferromanganese crusts are reversed toward less radiogenic signatures starting around 3–4 Ma, which is contemporaneous with the one order of magnitude dust flux increase to the central North Pacific. This decrease in ε_{Nd} during the past 3–4 Myr cannot be related to an increase in the North Atlantic Deep Water (NADW) component present in the Pacific Ocean at that time since NADW became a strong influence in the Pacific already in the late Miocene [*Rea et al.*, 1995; *Frank et al.*, 1999]. Moreover, *Frank et al.* [2002] have suggested that there was no change in ε_{Nd} in circumpolar deep water over the past 14 Myr, implying the absence of a NADW signal increase in the circumpolar current water mass. It is therefore concluded that if atmospheric fallout indeed provides a major source of seawater Nd as recently proposed [*Tachikawa et al.*, 1999; *Greaves et al.*, 1999], then the late Pliocene decrease in ε_{Nd} points to a resolvable but small contribution of dust-related Nd in response to the tenfold dust flux increase starting at circa 3.5 Ma. This conclusion is consistent with that of *Greaves et al.* [1999] who argued that atmospheric deposition of mineral dust from the Asian continent significantly affects the REE composition of modern seawater in the western Pacific Ocean. Since the eolian dust load over the entire central North Pacific is dominated by material from central Asia, all Pacific crusts show this reversal in trend starting at 3–4 Ma (Figure 5). Mass balance considerations then infer that eolian dust-bound Nd would have been an unimportant source for Pacific seawater Nd throughout the rest of the Cenozoic prior to 3–4 Ma. The Nd isotopic composition of

island arcs is nothing like that of Pacific seawater. Furthermore, unlike Pb, Nd is not an important component in volcanic aerosols. Therefore the Nd in Pacific seawater is dominated by dissolved Nd in riverine runoff as proposed by *Jones et al.* [1994].

5. Conclusions

[29] The eolian dust stratigraphy retrieved from giant piston core LL44-GPC3 in the central North Pacific shows two distinct intervals based on Nd and Pb isotopes. Prior to circa 40 Ma, the site of GPC3 was under the influence of Southern Hemisphere winds. A variable mixture of island arc volcanic material and continental dust from Central America was deposited from easterly trade winds south of the Intertropical Convergence Zone. In the late Eocene the Southern Hemisphere wind system extended far north of the equator (~20°N), consistent with sluggish atmospheric circulation, thus warm climate, in the Northern Hemisphere during the Eocene. In the late Eocene the Intertropical Convergence Zone migrated relatively southward; hence the GPC3 site came under the influence of Northern Hemisphere Winds. Smooth evolutionary trends in Nd isotopic compositions since circa 40 Ma are interpreted to monitor the progressive drying of central Asia, possibly triggered by the westward retreat of the paleo-Tethys [*Ramstein et al.*, 1997].

[30] The Pb isotopic composition of silicate dust and the flux of this component with time show no correlation with records of deep water Pb isotopic compositions as available in marine ferromanganese crusts. Therefore the Pb in Pacific deep water most likely originates from volcanic aerosols from island arcs, and the exchangeable Pb adherent to dust [*Jones et al.*, 2000] may have the same origin. If not, the contribution of eolian dust Pb to Pacific deep water is clearly subordinate since the one order of magnitude flux increase of eolian dust since circa 3.5 Ma had no effect.

[31] Comparison of time series of Nd isotopic compositions of Pacific deep water and dust flux suggest that dust-bound Nd became a resolvable source component only in the late Pliocene when dust flux to the central North Pacific was high. Dust-bound Nd therefore has made up a small fraction of the total dissolved Nd budget in the Pacific Ocean since the late Pliocene. If so, mass balance considerations infer that eolian dust was an unimportant source for Pacific deep water Nd prior to 3–4 Ma. Predominance of Asian dust in the central Pacific realm for the past 40 Myr is demonstrated and bears great potential in better constraining the tectonic and climatic evolution of this landmass and Pacific seawater chemistry alike, both of which are recorded in sediments from the central North Pacific Ocean.

Appendix A: Analytical Techniques

[32] For Nd isotopic analyses, samples were dissolved in ~0.2 *N* HNO_3 and diluted to ~120 ppb concentration after chemical purification, aiming at 3 V intensity on mass 144. In-run precision was of the order of 10 ppm for 100 ratios acquired in static mode. The measurement routine was set up in such a way that the measured $^{143}Nd/^{144}Nd$ ratio was corrected in two different ways for mass discrimination by using $^{146}Nd/^{144}Nd = 0.7219$ and $^{148}Nd/^{144}Nd = 0.24308$ [*Wasserburg et al.*, 1981] using a power law. Here $^{142}Nd/^{144}Nd$ and $^{150}Nd/^{144}Nd$ as normalizing ratios were not used because of possible isobaric interference of ^{142}Ce and ^{150}Sm. The 45 standard runs (JMC Nd) performed bracketing and in between the ~70 sample analyses revealed two noteworthy observations: First, the external reproducibility of the $^{143}Nd/^{144}Nd$ ratios normalized to $^{148}Nd/^{144}Nd$ was slightly better ($^{143}Nd/^{144}Nd = 0.511856 \pm 0.000022$) compared to that normalized to $^{146}Nd/^{144}Nd$ ($^{143}Nd/^{144}Nd = 0.511862 \pm 0.000026$); hence the data normalized to $^{148}Nd/^{144}Nd$ are reported here (all samples gave ≥150 mV on mass 148). Second, the external reproducibility we achieved during a single measurement session (two standard deviations absolute as good as 0.000012, determined on at least seven standard runs) was superior to that calculated over the entire period of analyses; hence we normalized the data of a single measurement session to the given ratio of $^{143}Nd/^{144}Nd = 0.511847$ [*Wasserburg et al.*, 1981]. In doing so, we achieved an external reproducibility of 0.4 ε_{Nd} at the two standard deviation level that is equivalent to that obtained by thermal ionization mass spectrometry (TIMS) [e.g., *Wasserburg et al.*, 1981] and by other MC-ICPMS instruments [*Luais et al.*, 1997]. Isobaric interferences of Sm were corrected for by monitoring mass 147 but were insignificant due to the quantitative separation of Nd from Sm during HDEHP chemistry.

[33] For Pb isotopic analyses, samples were dissolved in ~0.2 *N* HNO_3 and diluted to ~100 ppb after chemical purification, aiming at <4 V intensity on mass 208. Because Pb does not possess an invariant isotope ratio, mass discrimination was corrected for by using NIST SRM-997 Tl ($^{203}Tl/^{205}Tl = 2.3871$ certified value [*Dunstan et al.*, 1980]) that was added to the samples prior to analysis [*Longerich et al.*, 1987] and a power law. As for Nd, 23 standard analyses (mixed solution containing ~100 ppb NIST SRM-981 Pb and ~80 ppb NIST SRM-997 Tl) were performed bracketing and between the ~30 sample analyses. Isobaric interferences of Hg on mass 204 were below 1‰ and corrected for by using $^{204}Hg/^{202}Hg = 0.2301$ [*Subcommittee for the isotopic composition of the elements* (*SIAM*), 1991]. In-run precision for $^{206,207,208}Pb/^{204}Pb$ ratios is around 140 ppm for 100 ratios acquired in static mode. This is worse compared to the in-run precision of ~30 ppm obtained for Nd because the maximum allowed intensity of 4 V on mass 208 restricted the intensity on mass 204 to below ~100 mV. In-run precisions for $^{207}Pb/^{206}Pb$ and $^{208}Pb/^{206}Pb$ were 22 and 42 ppm, respectively, of the order of that obtained for Nd. The external reproducibility at the two standard deviation level over the entire period of sample analyses was $^{206}Pb/^{204}Pb = 16.9369 \pm 0.0021$, $^{207}Pb/^{204}Pb = 15.4882 \pm 0.0020$, $^{208}Pb/^{204}Pb = 36.6784 \pm 0.0053$, $^{207}Pb/^{206}Pb = 0.91446 \pm 0.00002$, and $^{208}Pb/^{206}Pb = 2.16558 \pm 0.00009$ ($n = 23$). When compared to the Pb isotope ratios obtained by *Todt et al.* [1996], we note that $^{208}Pb/^{204}Pb$ and $^{208}Pb/^{206}Pb$ ratios are significantly lower, whereas the $^{206}Pb/^{204}Pb$, $^{207}Pb/^{204}Pb$, and $^{207}Pb/^{206}Pb$ ratios agree within error. The deviation of isotopic ratios involving mass 208 could be explained by a nonlinearity in gain of the Faraday detector

above 3 V intensity. The standards were intentionally run at intensities of 3–4 V on mass 208 in order to improve the signal-to-noise ratio on mass 204, which was the limiting factor for the reproducibility of isotopic ratios involving ^{204}Pb when samples were run at ^{208}Pb = 3 V [*Rehkämper and Halliday*, 1998]. When corrected for mass discrimination with ^{203}Tl/^{205}Tl = 2.3885 as proposed by *Rehkämper and Halliday* [1999] instead of the certified value of 2.3871 and compared with the values of *Todt et al.* [1996], all isotopic compositions involving ^{204}Pb are significantly higher, while the ^{207}Pb/^{206}Pb and ^{208}Pb/^{206}Pb agree just within error. We therefore chose to report all our measurements normalized to the certified isotopic composition of Tl (^{203}Tl/^{205}Tl = 2.3871) because discrepancies in isotopic compositions when compared to the values of *Todt et al.* [1996] can plausibly be explained.

[34] **Acknowledgments.** This study was supported by the Department of Energy. T.P. thanks D.-C. Lee for thorough introduction to MC-ICPMS analysis. We appreciate discussions with Martin Frank on earlier versions of this manuscript, the constructive anonymous review, and the comments by the associate editor.

References

Abouchami, W., S. L. Goldstein, S. J. G. Galer, A. Eisenhauer, and A. Mangini, Secular changes of lead and neodymium in central Pacific seawater recorded by a Fe-Mn, *Geochim. Cosmochim. Acta*, *61*, 3957–3974, 1997.

Christensen, J. N., A. N. Halliday, L. V. Godfrey, J. R. Hein, and D. K. Rea, Climate and ocean dynamics and the lead isotopic records in Pacific ferromanganese crusts, *Science*, *277*, 913–918, 1997.

Corliss, B. H., and C. D. Hollister, A palaeoenvironmental model for Cenozoic sedimentation in the central North Pacific, in *The Ocean Floor*, edited by R. A. Scrutton and M. Talwani, pp. 277–304, John Wiley, New York, 1982.

Ding, Z., Z. Yu, N. W. Rutter, and T. Liu, Towards an orbital time-scale for Chinese loess deposits, *Quat. Sci. Rev.*, *13*, 39–70, 1994.

Doyle, P. S., and W. R. Riedel, Cretaceous to Neogene Ichthyoliths in a giant piston core from the central North Pacific, *Micropaleontology*, *25*, 337–364, 1980.

Dunstan, L. P., J. W. Gramlich, I. L. Barnes, and W. C. Purdy, Absolute isotopic abundance and the atomic weight of a reference sample of thallium, *J. Res. Natl. Bur. Stand.*, *85*, 1–10, 1980.

Flohn, H., A hemispheric circulation asymmetry during late Tertiary, *Geol. Rundsch.*, *70*, 725–736, 1981.

Francis, P. W., and C. J. Hawkesworth, Late Cenozoic rates of magmatic activity in the central Andes and their relationships to continental crust formation and thickening, *J. Geol. Soc. London*, *151*, 845–854, 1994.

Frank, M., B. C. Reynolds, and R. K. O'Nions, Nd and Pb isotopes in Atlantic and Pacific water masses before and after closure of the Panama gateway, *Geology*, *27*, 1147–1150, 1999.

Frank, M., N. Whiteley, S. Kasten, J. R. Hein, and R. K. O'Nions, North Atlantic Deep Water export to the Southern Ocean over the past 14 Myr: Evidence from Nd and Pb isotopes in ferromanganese crusts, *Paleoceanography*, *17*(2), 10.1029/2000PA000606, 2002.

Goldstein, S. L., R. K. O'Nions, and P. J. Hamilton, A Sm-Nd isotopic study of atmospheric dusts and particulates from major river systems, *Earth Planet. Sci. Lett.*, *70*, 221–236, 1984.

Gottfried, M. D., P. S. Doyle, and W. R. Riedel, Advances in Ichthyolith stratigraphy of the Pacific Neogene and Oligocene, *Micropaleontology*, *30*, 71–85, 1984.

Greaves, M. J., H. Elderfield, and E. R. Sholkovitz, Aeolian sources of rare earth elements to the western Pacific Ocean, *Mar. Chem.*, *68*, 31–38, 1999.

Grousset, F. E., P. E. Biscaye, A. Zindler, J. Prospero, and R. Chester, Neodymium isotopes as tracers in marine sediments and aerosols: North Atlantic, *Earth Planet. Sci. Lett.*, *87*, 367–378, 1988.

Halliday, A. N., et al., Applications of multiple collector-ICPMS to cosmochemistry, geochemistry, and paleoceanography, *Geochim. Cosmochim. Acta*, *62*, 919–940, 1998.

Hay, W. W., et al., Alternative global Cretaceous paleogeography, in *The Evolution Of Cretaceous Ocean/Climate Systems*, edited by E. Barrera and C. Johnson, *Spec. Pap. Geol. Soc. Am.*, *332*, 1–47, 1999.

Jahn, B. M., and K. C. Condie, Evolution of the Kaapvaal-craton as viewed from geochemical and Sm-Nd isotopic analyses of intracratonic pelites, *Geochim. Cosmochim. Acta*, *59*, 2239–2258, 1995.

Janecek, T. R., and D. K. Rea, Eolian deposition in the northeast Pacific Ocean: Cenocoic history of atmospheric circulation, *Geol. Soc. Am. Bull.*, *94*, 730–738, 1983.

Jones, C. E., A. N. Halliday, D. K. Rea, and R. M. Owen, Neodymium isotopic variations in North Pacific modern silicate sediment and the insignificance of detrital REE contributions to seawater, *Earth Planet. Sci. Lett.*, *127*, 55–66, 1994.

Jones, C. E., A. N. Halliday, D. K. Rea, and R. M. Owen, Eolian inputs of lead to the North Pacific, *Geochim. Cosmochim. Acta*, *64*, 1405–1416, 2000.

Kutzbach, J. E., W. L. Prell, and W. F. Ruddiman, Sensitivity of Eurasian climate to surface uplift of the Tibetan Plateau, *J. Geol.*, *101*, 177–190, 1993.

Kyte, F. T., and J. T. Wasson, Accretion rate of extraterrestrial matter—Iridium deposited 33 to 67 million years ago, *Science*, *232*, 1225–1229, 1986.

Kyte, F. T., M. Leinen, G. R. Heath, and L. Zhou, Cenozoic sedimentation history of the central North Pacific: Inferences from the elemental geochemistry of core LL44-GPC3, *Geochim. Cosmochim. Acta*, *57*, 1719–1740, 1993.

Lee, D.-C., and A. N. Halliday, Hafnium-tungsten chronometry and the timing of terrestrial core formation, *Nature*, *378*, 771–774, 1995.

Lee, D.-C., et al., Hafnium isotope stratigraphy of ferromanganese crusts, *Science*, *285*, 1052–1054, 1999.

Leinen, M., The origin of paleochemical signatures in North Pacific pelagic clays: Partitioning experiments, *Geochim. Cosmochim. Acta*, *51*, 305–319, 1987.

Leinen, M., and G. R. Heath, Sedimentary indicators of atmospheric activity in the Northern Hemisphere during the Cenozoic, *Palaeogeogr. Palaeoclimatol. Palaeoecol.*, *36*, 1–21, 1981.

Ling, H. F., et al., Evolution of Nd and Pb isotopes in central Pacific seawater from ferromanganese crusts, *Earth Planet. Sci. Lett.*, *146*, 1–12, 1997.

Longerich, H. P., B. J. Fryer, and D. F. Strong, Determination of lead isotope ratios by inductively coupled plasma-mass spectrometry (ICP-MS), *Spectrochim. Acta, Part B*, *42*, 39–48, 1987.

Luais, B., P. Telouk, and F. Albarede, Precise and accurate neodymium isotopic measurements by plasma-source mass spectrometry, *Geochim. Cosmochim. Acta*, *61*, 4847–4854, 1997.

McLennan, S. M., S. R. Taylor, M. T. McCulloch, and J. B. Maynard, Geochemical and Nd-Sr isotopic composition of deep-sea turbidites: Crustal evolution and plate tectonic associations, *Geochim. Cosmochim. Acta*, *54*, 2015–2050, 1990.

Merrill, J. T., M. Uematsu, and R. Bleck, Meteorological analysis of long range transport of mineral aerosols over the North Pacific, *J. Geophys. Res.*, *94*, 8584–8598, 1989.

Nakai, S., A. N. Halliday, and D. K. Rea, Provenance of dust in the Pacific Ocean, *Earth Planet. Sci. Lett.*, *119*, 143–157, 1993.

Nozaki, Y., J. Thompson, and K. K. Turekian, The distribution of ^{210}Pb and ^{210}Po in the surface waters of the Pacific Ocean, *Earth Planet. Sci. Lett.*, *32*, 304–312, 1976.

Patterson, C. C., and D. M. Settle, Review of data on eolian fluxes of industrial and natural lead to the lands and seas in remote regions on a global scale, *Mar. Chem.*, *22*, 137–162, 1987a.

Patterson, C. C., and D. M. Settle, Magnitude of lead flux to the atmosphere from volcanoes, *Geochim. Cosmochim. Acta*, *51*, 675–681, 1987b.

Petford, N., M. P. Atherton, and A. N. Halliday, Rapid magma production rates, underplating and remelting in the Andes: Isotopic evidence from northern-central Peru (9–11 degrees S), *J. S. Am. Earth Sci.*, *9*, 69–78, 1996.

Pettke, T., A. N. Halliday, C. M. Hall, and D. K. Rea, Dust production and deposition in Asia and the North Pacific Ocean over the past 12 Myr, *Earth Planet. Sci. Lett.*, *178*, 397–413, 2000.

Prince, R. A., G. R. Heath, and M. Kominz, Paleomagnetic stratigraphies of central North Pacific sediment cores: Stratigraphy, sedimentation rates and the origin of magnetic instability, *Geol. Soc. Am. Bull.*, *91*, 1789–1835, 1980.

Prueher, L. M., and D. K. Rea, Tephrochronology of the Kamchatka-Kurile and Aleutian

arcs: Evidence for volcanic episodicity, *J. Volcanol. Geotherm. Res.*, *106*, 67–84, 2001.

Ramstein, G., F. Fluteau, J. Besse, and S. Joussaume, Effect of orogeny, plate motion and land sea distribution on Eurasian climate change over the past 30 million years, *Nature*, *386*, 788–795, 1997.

Rea, D. K., The paleoclimatic record provided by eolian deposition in the deep sea: The geologic history of wind, *Rev. Geophys.*, *32*, 159–195, 1994.

Rea, D. K., M. Leinen, and T. R. Janecek, Geologic approach to the long-term history of atmospheric circulation, *Science*, *227*, 721–725, 1985.

Rea, D. K., I. A. Basov, L. A. Krissek, and L. S. Party, Scientific results of drilling the north Pacific transect, *Proc. Ocean Drill. Program Sci. Results*, *145*, 577–596, 1995.

Rea, D. K., H. Snoeckx, and L. H. Joseph, Late Cenozoic eolian deposition in the North Pacific: Asian drying, Tibetan uplift, and cooling of the Northern Hemisphere, *Paleoceanography*, *13*, 215–224, 1998.

Rehkämper, M., and A. N. Halliday, Accuracy and long-term reproducibility of lead isotopic measurements by multiple-collector inductively coupled plasma mass spectrometry using an external method for correction of mass discrimination, *Int. J. Mass Spectrom.*, *181*, 123–133, 1998.

Rehkämper, M., and A. N. Halliday, The precise measurement of Tl isotopic compositions by MC-ICPMS: Application to the analysis of geological materials and meteorites, *Geochim. Cosmochim. Acta*, *63*, 935–944, 1999.

Schaule, B. K., and C. C. Patterson, Lead concentrations in the northeast Pacific: Evidence for global anthropogenic perturbations, *Earth Planet. Sci. Lett.*, *54*, 97–116, 1981.

Subcommittee for the isotopic composition of the elements (SIAM), Isotopic compositions of the elements 1989, *Pure Appl. Chem.*, *63*, 992–1003, 1991.

Sigurdsson, H., S. P. Kelley, S. N. Carey, The Cenozoic record of Caribbean explosive volcanism: $^{40}Ar/^{39}Ar$ dating of tephra, *Eos Trans. AGU*, 79(17), Spring Meet. Suppl., S172, 1998.

Sims, K. W. W., et al., Mechanisms of magma generation beneath Hawaii and midocean ridges—Uranium/thorium and samarium/neodymium isotopic evidence, *Science*, *267*, 508–512, 1995.

Tachikawa, K., C. Jeandel, and M. Roy-Barman, A new approach to the Nd residence time in the ocean: The role of atmospheric inputs, *Earth Planet. Sci. Lett.*, *170*, 433–446, 1999.

Taylor, S. R., S. M. McLennan, and M. T. McCulloch, Geochemistry of loess, continental crustal composition and crustal model ages, *Geochim. Cosmochim. Acta*, *47*, 1897–1905, 1983.

Todt, W., R. A. Cliff, A. Hanser, and A. W. Hofmann, Evaluation of a ^{202}Pb-^{205}Pb double spike for high-precision lead isotope analysis, in *Earth Processes*: *Reading the Isotopic Code, Geophys. Monogr. Ser.*, vol. 95, pp. 429–437, AGU, Washington, D. C., 1996.

van Andel, T. H., G. R. Heath, and T. C. Moore, Cenozoic history and paleoceanography of the central equatorial Pacific, *Mem. Geol. Soc. Am.*, *143*, 1–134, 1975.

von Blanckenburg, F., and H. Igel, Lateral mixing and advection of reactive isotope tracers in ocean basins: Observations and mechanisms, *Earth Planet. Sci. Lett.*, *169*, 113–128, 1999.

von Blanckenburg, F., R. K. O'Nions, and J. R. Hein, Distribution and sources of pre-anthropogenic lead isotopes in deep ocean water from Fe-Mn crusts, *Geochim. Cosmochim. Acta*, *60*, 4957–4963, 1996.

Walker, J. A., et al., Abrupt change in magma generation processes across the central-American arc in southeastern Guatemala—Flux dominated melting near the base of the wedge to decompression melting near the top of the wedge, *Contrib. Mineral. Petrol.*, *120*, 378–390, 1995.

Wark, D. A., Oligocene ash flow volcanism, northern Sierra-Madre Occidental: Role of mafic and intermediate-composition magmas in rhyolite genesis, *J. Geophys. Res.*, *96*, 13,389–13,411, 1991.

Wasserburg, G. J., S. B. Jacobsen, D. J. DePaolo, M. T. McCulloch, and T. Wen, Precise determination of Sm/Nd ratios, Sm and Nd isotopic abundances in standard solutions, *Geochim. Cosmochim. Acta*, *45*, 2311–2323, 1981.

A. N. Halliday and T. Pettke, ETH Zürich, Isotope Geochemistry and Mineral Resources, ETH Zentrum NO, CH-8092 Zürich, Switzerland. (thomas.pettke@erdw.ethz.ch)

D. K. Rea, Department of Geological Sciences, University of Michigan, Ann Arbor, MI, 48109-1063, USA.